ORIGINAL PAPER

Evaluation of thermal bioclimate based on observational data and numerical simulations: an application to Greece

**Theodore M. Giannaros · Dimitrios Melas ·
Andreas Matzarakis**

Abstract The evaluation of thermal bioclimate can be conducted employing either observational or modeling techniques. The advantage of the numerical modeling approach lies in that it can be applied in areas where there is lack of observational data, providing a detailed insight on the prevailing thermal bioclimatic conditions. However, this approach should be exploited carefully since model simulations can be frequently biased. The aim of this paper is to examine the suitability of a mesoscale atmospheric model in terms of evaluating thermal bioclimate. For this, the numerical weather prediction Weather Research and Forecasting (WRF) model and the radiation RayMan model are employed for simulating thermal bioclimatic conditions in Greece during a 1-year time period. The physiologically equivalent temperature (PET) is selected as an index for evaluating thermal bioclimate, while synoptic weather station data are exploited for verifying model performance. The results of the present study shed light on the strengths and weaknesses of the numerical modeling approach. Overall, it is shown that model simulations can provide a useful alternative tool for studying thermal bioclimate. Specifically for Greece, the WRF/RayMan modeling system was found to perform adequately well in reproducing the spatial and temporal variations of PET.

Keywords WRF · RayMan · Numerical modeling ·
Physiologically equivalent temperature · Thermal
bioclimate · Greece

T. M. Giannaros (✉) · D. Melas
Laboratory of Atmospheric Physics, School of Physics, Aristotle
University of Thessaloniki, 54124 Thessaloniki, Greece
e-mail: thgian@auth.gr

A. Matzarakis
Chair of Meteorology and Climatology, Albert-Ludwigs University
of Freiburg, Werthmannstrasse 10, 79085 Freiburg, Germany

Introduction

The thermal bioclimate is of great interest not only for the stakeholders involved in the public health and tourism sectors (De Freitas et al. 2007), but also for the general public. It comprises the meteorological parameters of air temperature and humidity, wind speed, and short- and long-wave radiation fluxes, which thermophysiologically influence human beings both indoors and outdoors (Höppe 1993). The thermal bioclimate is significant for human health due to the close relationship between the thermoregulatory mechanism and the circulatory system (Höppe 1993; Nastos and Matzarakis 2006).

The evaluation of the thermal bioclimate is typically conducted using appropriate indices. The concept is that the factors that influence human response to the thermal environment are integrated to provide a single index value (Fanger 1972; Parsons 1993). In the past, simple thermal indices were frequently used for assessing the thermal bioclimate. Such indices (e.g., ISO 1982; Steadman 1971; Thom 1959) are nowadays considered to be inadequate for describing the thermal environment. This is because they are based on single or composite meteorological parameters and do not account for the thermal physiology (Höppe 1993; Mayer 1993).

The above limitations can be eliminated by using physiologically relevant indices that are derived from the human energy balance for the assessment of the thermal environment (Höppe 1993). Such indices are the physiologically equivalent temperature (PET; Mayer and Höppe 1987) or standard effective temperature (SET*; Gagge et al. 1986; Höppe 1999; Mayer 1993) and the predicted mean vote (PMV; Fanger 1972). Thermophysiologically significant indices can be computed at varying time and spatial resolutions, providing different levels of information at each case. At the microscale (0–500 m), the implementation of these indices can be particularly useful for urban planning purposes and heat health

issues. For instance, Gulyás et al. (2006) used PET to conduct a human-biometeorological assessment of the microclimate of a complex urban district in the city of Szeged, Hungary. More recently, Fröhlich and Matzarakis (2013) used the same index for evaluating the impact of urban street design and surface materials on the thermal bioclimate of a public place in the city of Freiburg, Germany. Charalampopoulos et al. (2013) also applied PET to investigate the variation of human thermal comfort in selected urban areas with different vegetation and building structures, in Athens, Greece.

On the other hand, there is a growing demand for temporally and spatially detailed thermal bioclimate data, which could be used for applied research in the field of tourism climatology (Matzarakis 2006; Shiue and Matzarakis 2011). This demand can be met by means of constructing bioclimatic maps that depict the spatial distribution of thermophysiologically significant indices at the mesoscale (≥1 km). Spatially detailed bioclimatic data can be derived from point data with the aid of geostatistical methods (Matzarakis and Mayer 1997). However, this approach has some limitations. More importantly, the accuracy of this method depends strongly on the availability of point data (i.e., observations). This is because it employs multiple linear regression methods for determining the relationship between the dependent variable (i.e., the selected index) and a set of independent variables (e.g., geographic location, elevation, land use, etc.) (Matzarakis and Mayer 1997). Therefore, it is in principle required that the available point data be representative of the entire area over which the geostatistical approach is implemented.

Numerical modeling can provide an alternative solution for studying the temporal and spatial variations of the thermal bioclimate. Cross-scale atmospheric modeling systems, which are able to simulate meteorological conditions from regional to building scales and which can be coupled to human-response models, are considered to be a valuable tool for this purpose. The key advantage of numerical models is that they can provide detailed meteorological data at the desired temporal and spatial resolution for, literally, any geographical area of interest. These data can be consequently exploited for evaluating the thermal bioclimate, especially in areas where there is lack of high quality measurements. Moreover, numerical models can serve as an important tool for assessing the thermal bioclimatic impact of future climate change (e.g., Endler and Matzarakis 2011; Fröhlich and Matzarakis 2013) and examining the effect of potential mitigation strategies (e.g., Papangelis et al. 2012).

The key objective of the present study is to examine the degree to which a mesoscale numerical weather prediction (NWP) model can be used for driving a human-response model in order to evaluate the thermal bioclimate. The study area, Greece, was selected due to its complex topography that may result to considerable variations of the thermal

bioclimatic conditions at different locations (Matzarakis and Mayer 1997). Furthermore, this study extends to an entire year to allow for a complete evaluation of the seasonal variations of the thermal environment.

Materials and methods

Study area and meteorological data

Greece is located in southeast Europe (Fig. 1a), confined to the area between 34° and 42° northern latitude and 19° and 28° eastern longitude. It covers about 132,000 km², comprising a mountainous, peninsular mainland jutting out into the southeast Mediterranean at the southern end of the Balkans. The topography of Greece is very complex and highly variable (Fig. 1b). Although it has one of the longest coastlines in the world, due to its highly indented coastline and numerous islands, it is also one of the most mountainous countries in Europe (CIA 2013).

The observational data used in the present study were obtained from a network of 19 surface synoptic weather stations, operated by the Hellenic National Meteorological Service (HNMS) and part of the World Meteorological Organization (WMO) weather station network. The locations of the stations are shown in Fig. 1b, while Table 1 summarizes basic information about the measuring sites. It should be mentioned that all weather stations used in this study are located on planar areas and close to the coastline, except from station 16648 that is found at an inland site (Fig. 1b). Data availability justifies the selection of this particular set of measuring sites. The data used cover a 1-year period, spanning from January 1 through December 31 2003.

Physiologically equivalent temperature

The physiologically equivalent temperature (PET) was used as an index for assessing the thermal bioclimate (Höppe 1999). It has been widely used as an index for studying the thermal bioclimate, and thus, comparisons with past studies can be easily made. The calculation of PET is based on a human energy balance model, namely the Munich Energy Balance Model for Individuals (MEMI, Höppe 1984).

Implemented models

The study of the thermal bioclimate of Greece was conducted using a combination of two models. The NWP Weather Research and Forecasting (WRF) model (Skamarock et al. 2008) was employed for the numerical simulation of meteorological conditions, while PET was computed by applying the RayMan model (Matzarakis et al. 2007, 2010).
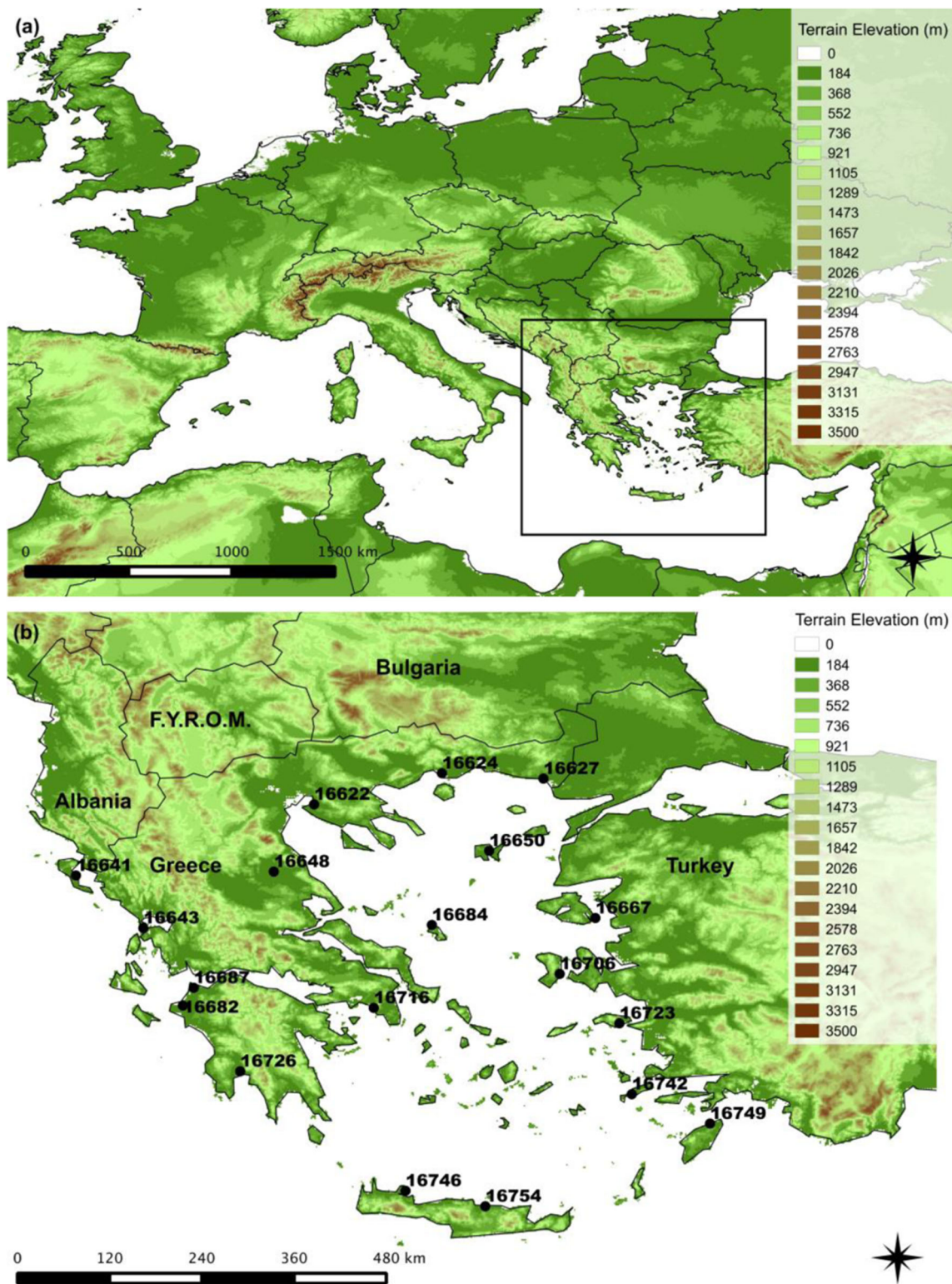
Fig. 1 Topographic map of **a** Europe with identification of Greece (*black box*) and **b** Greece with identification of the surface synoptic weather stations (dots and World Meteorological Organization IDs)

WRF

The meteorological model used in this study is the WRF-ARW (Advanced Research Weather), version 3.2

(Skamarock et al. 2008). The numerical simulations were conducted on one modeling domain with horizontal grid resolution of 6 km (mesh size of 260×165), focusing on Greece (Fig. 1a). Thirty-three vertical levels were defined

Table 1 Summary of the characteristics of the 19 surface synoptic weather stations, grouped by geographical region

WMO ID	Site	Latitude (°N)	Longitude (°E)	Altitude (asl)
West Greece				
16643	Aktion	38.92	20.77	1.00
16682	Andravida	37.92	21.28	15.10
16687	Araxos	38.15	21.42	11.70
16726	Kalamata	37.07	22.02	11.10
16641	Kerkira	39.60	19.90	4.00
North Greece				
16627	Alexandroupolis	40.85	25.93	3.50
16624	Chrissoupolis	40.52	22.97	4.80
16622	Thessaloniki	40.92	24.62	3.00
Central Greece				
16648	Larissa	39.65	22.45	74.00
South Greece				
16716	Athens	37.89	23.74	15.00
North Aegean				
16650	Limnos	39.92	25.23	4.60
Central Aegean				
16706	Chios	38.33	26.14	3.80
16667	Mitilini	39.05	26.60	5.00
16723	Samos	37.69	26.91	7.30
16684	Skiros	38.96	24.49	17.90
South Aegean				
16754	Heraklion	35.33	25.18	39.00
16742	Kos	36.78	27.07	125.00
16749	Rodos	36.40	28.08	11.50
16746	Souda	35.53	24.15	151.60

asl above sea level

and the model top was specified at 100 hPa. The physical options used for conducting the numerical simulations are summarized in Table 2.

The WRF simulations were initialized using the 0.25°× 0.25° spatial resolution and 6 h temporal resolution operational atmospheric analysis surface and pressure level data of the European Centre for Medium-range Weather Forecasts (ECMWF). The lateral boundary conditions for the modeling domain were obtained by linearly interpolating the ECMWF analysis data. The National Centre for Environmental Predictions (NCEP) ADP Operational Global Synoptic and Upper Air database was used for retrieving observational data for assimilation, at 6 h temporal resolution. Data assimilation was carried out using the advanced three-dimensional variational data assimilation system of WRF (WRF-Var, Skamarock et al. 2008).

Numerical simulations were conducted for the year 2003. The simulations were initialized at 0000 UTC every 9 days,

Table 2 Summary of the physical options (schemes) used in the numerical simulations

Physics	Parameterization (scheme)	Reference
Surface layer	ETA	Janjic (1996, 2002)
Planetary boundary layer	MYJ (Mellor-Yamada-Janjic)	Janjic (1994)
Land surface model	Noah	Chen and Dudhia (2001)
Short-wave radiation	Dudhia	Dudhia (1989)
Long-wave radiation	RRTM (Rapid Radiative Transfer Model)	Mlawer et al. (1997)
Cumulus	Kain-Fritsch	Kain (2004)
Microphysics	WRF Single-Moment 6-Class	Hong and Lim (2006)

integrating for 10 days. The first 24 h of each simulation was discarded as coinciding with the model's spin-up period. Data assimilation was first carried out at the beginning of each 10-day integration time period (cold model start) and at 6 h intervals, thereafter (cycling model run).

RayMan

RayMan is a numerical model that allows for the computation of radiation fluxes in simple and complex environments (Matzarakis et al. 2007, 2010). This enables the computation of the mean radiant temperature that is necessary for the calculation of thermal bioclimatic indices, such as PET. The principal idea of this study was to implement RayMan twice to calculate PET at the locations of the synoptic weather station stations (Fig. 1b). During the first implementation, RayMan was driven by the in situ meteorological data. During the second, the WRF-simulated meteorological data, bilinearly interpolated onto the measuring sites, were used. Bilinear interpolation was selected as a common approach in similar studies focusing on model performance evaluation (e.g., Giannaros et al. 2013a; Miao et al. 2007). At both cases, air temperature, vapor pressure, wind speed, and cloud cover data were used for driving RayMan. The resulting PET values were classified into nine classes of thermal stress (Table 3; Matzarakis and Mayer 1996) and analyzed.

Results

Validation of the meteorological model

Domain-wide statistics provide an overall performance measure on how well the model simulations replicate the observed thermal bioclimatic conditions in Greece. Table 4 is a compilation of the computed model performance metrics for PET. The first categorization of the statistical measures is seasonal.

Table 3 Thermal stress classes for human beings [internal heat production of 80 W and heat transfer resistance of the clothing of 0.9 clo (clothing value)] after Matzarakis and Mayer (1996)

PET (°C)	Thermal perception	Level of thermal stress
<4	Very cold	Extreme cold stress
4–8	Cold	Strong cold stress
8–13	Cool	Moderate cold stress
13–18	Slightly cool	Slight cold stress
18–23	Comfortable	No thermal stress
23–29	Slightly warm	Slight heat stress
29–35	Warm	Moderate heat stress
35–41	Hot	Strong heat stress
>41	Very hot	Extreme heat stress

Table 4 Model performance metrics computed for PET for various subsets of data

Data subsets	PET (°C)		
	MBE	RMSE	R^2
Seasonal			
DJF	−0.29	2.30	0.84
MAM	−0.60	3.11	0.88
JJA	−1.31	3.82	0.80
SON	−0.24	2.80	0.86
Regional			
West Greece	−0.04	3.12	0.93
North Greece	−0.96	3.24	0.94
Central Greece	−0.22	3.32	0.94
South Greece	−1.63	2.87	0.98
North Aegean	0.32	2.89	0.95
Central Aegean	−0.94	3.11	0.93
South Aegean	−0.61	2.90	0.91

DJF December-January-February, *MAM* March-April-May, *JJA* June-July-August, *SON* September-October-November

For all seasons, the model simulations appear to be biased cold, underestimating PET by −0.24 °C in the autumn to −1.31 °C in the summer. Overall, the model seems to perform better during the cold half of the year (SON and DJF) than during the warm half (MAM and JJA). The best model observation agreement occurs in the winter, whereas the largest MBE and RMSE values were computed for the summer.

The second group of statistics (regional) in Table 4 was calculated from data subsets over the different regions of Greece for the entire study period. The model is found to be generally biased cold, underestimating PET by −0.04 °C over West Greece to −1.63 °C over South Greece. Not surprisingly, the presented statistical measures indicate a regional dependence of the model performance. In particular, it is clear that PET is better simulated over the regions of the Aegean Sea than over continental Greece. This could be, at least partially, attributed to the complex topography of continental Greece that is hard to model despite the relatively high horizontal resolution (6 km) that was specified.

Figure 2 depicts the relationship between the hourly model-simulated and observed PET during winter and summer for all examined stations. The previously identified underestimation (Table 4) is also obvious in Fig. 2. However, it now becomes clear that the model mainly underestimates the higher PET values. Despite the scattering of the data points, the correlation between modeled and observed PET is found to be good, showing statistically significant (α=0.05) R^2 values of 0.84 in winter (Fig. 2a) and 0.80 in summer (Fig. 2b). The greater scattering found for summer (Fig. 2b) could be due to the greater variability of meteorological conditions (e.g., cloud

Fig. 2 Scatter plots between observed (SYNOP) and model-simulated (WRF) hourly PET for **a** winter and **b** summer. The entire dataset (all stations) of each season has been used. The *red line* depicts the implemented linear least-square fit. Statistical parameters are presented within the plot. The number of observations-model pairs used is denoted with letter *N*
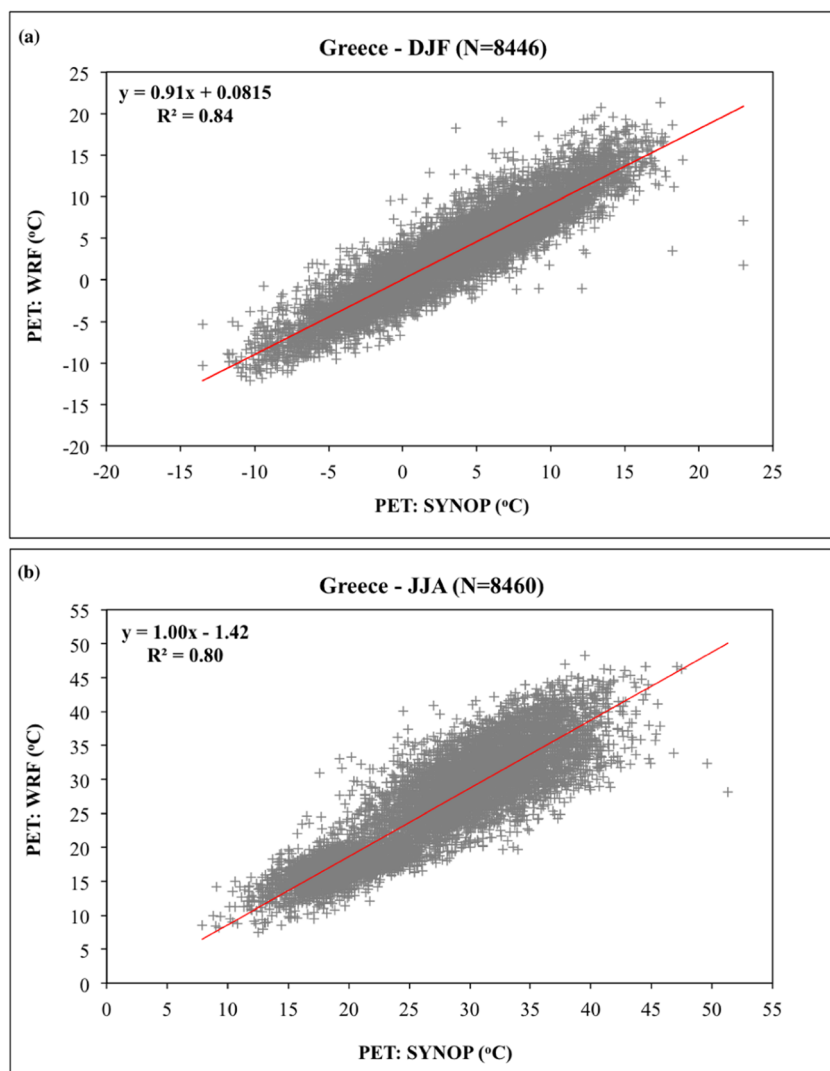
cover, wind), which is thought to cause variation in the simulation of thermal bioclimatic conditions (Matzarakis et al. 2007). In addition, the high complexity of the study area may also contribute to the observed differences, as the model simulations may not replicate accurately the local-scale meteorological conditions. Nevertheless, the overall agreement between the modeled and measured PET is found to be satisfactory.

Evaluation of thermal bioclimate of Greece

Two types of diagrams were used for assessing the thermal bioclimatic conditions at the selected synoptic weather stations. First, the hourly data were used for computing relative frequencies of PET classes on a monthly basis and constructing the bioclimatic diagrams for each examined region. These diagrams are advantageous in that they provide valuable information on the seasonal variation of the thermal bioclimatic conditions. In addition, time series diagrams of the daily PET

at 1200 UTC were constructed. The advantage of these diagrams is that they allow for an easy analysis of extreme values. The selected time of the day for constructing the time series of PET is justified by that it represents the most favorable thermal conditions during winter and the worst in summer.

Bioclimatic and time series diagrams were constructed for all regional groups of stations. For clarity, however, we present only those referring to the North and South Greece and the North and South Aegean. This particular selection enables us to investigate the geographical gradient and regional dependence of bioclimatic conditions in Greece. Nevertheless, it should be noted that similar findings were also obtained for the remaining regional groups of stations.

The numerical simulations, in agreement with the observations, indicate a typical seasonal variation of PET during the examined yearly period. As seen in Figs. 3 and 4, cold stress conditions (PET<13 °C) dominate from about November until April, whereas heat stress (PET>29 °C) is found to frequently occur in the summer. Interestingly, the summer

Fig. 3 Thermal bioclimate diagrams for North Greece: **a** observed and **b** modeled; South Greece: **c** observed and **d** modeled. Monthly frequencies were computed using the hourly PET data
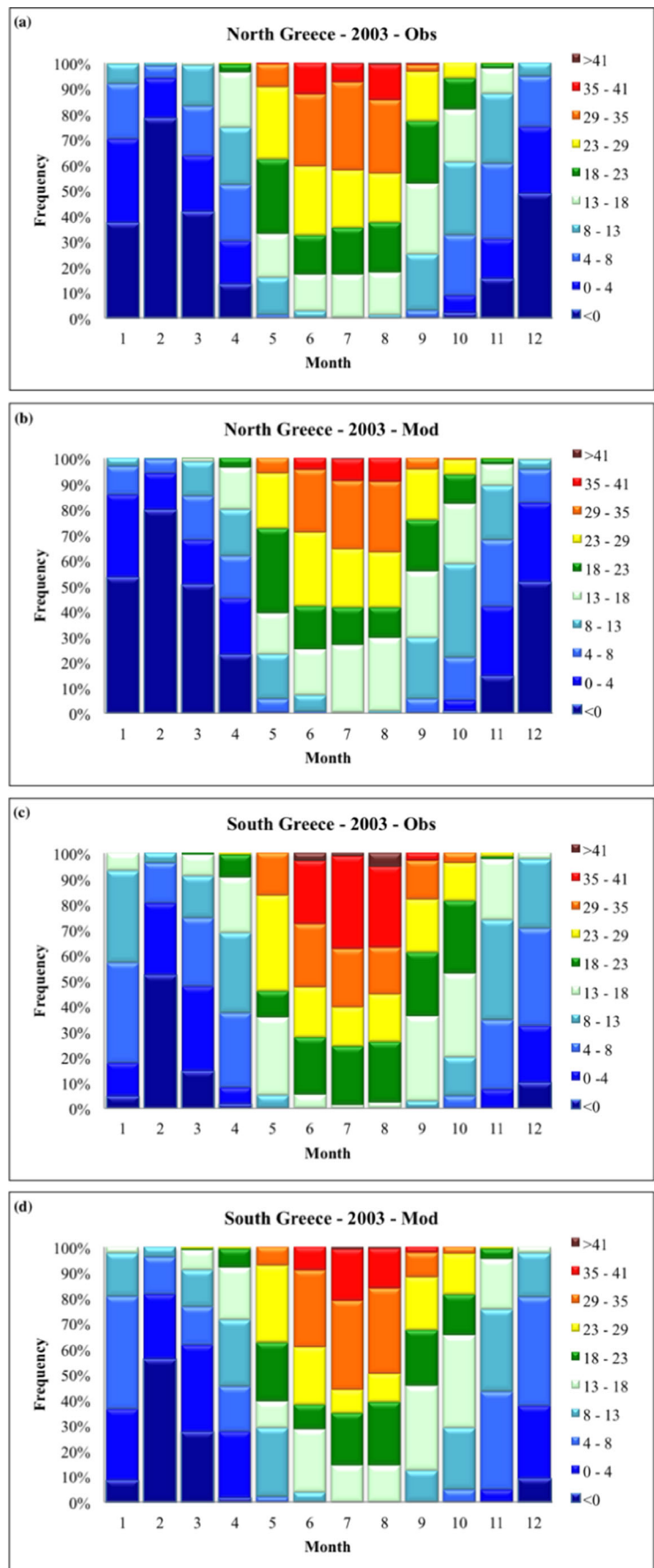
Fig. 4 Thermal bioclimate diagrams for North Aegean: **a** observed and **b** modeled; South Aegean: **c** observed and **d** modeled. Monthly frequencies were computed using the hourly PET data
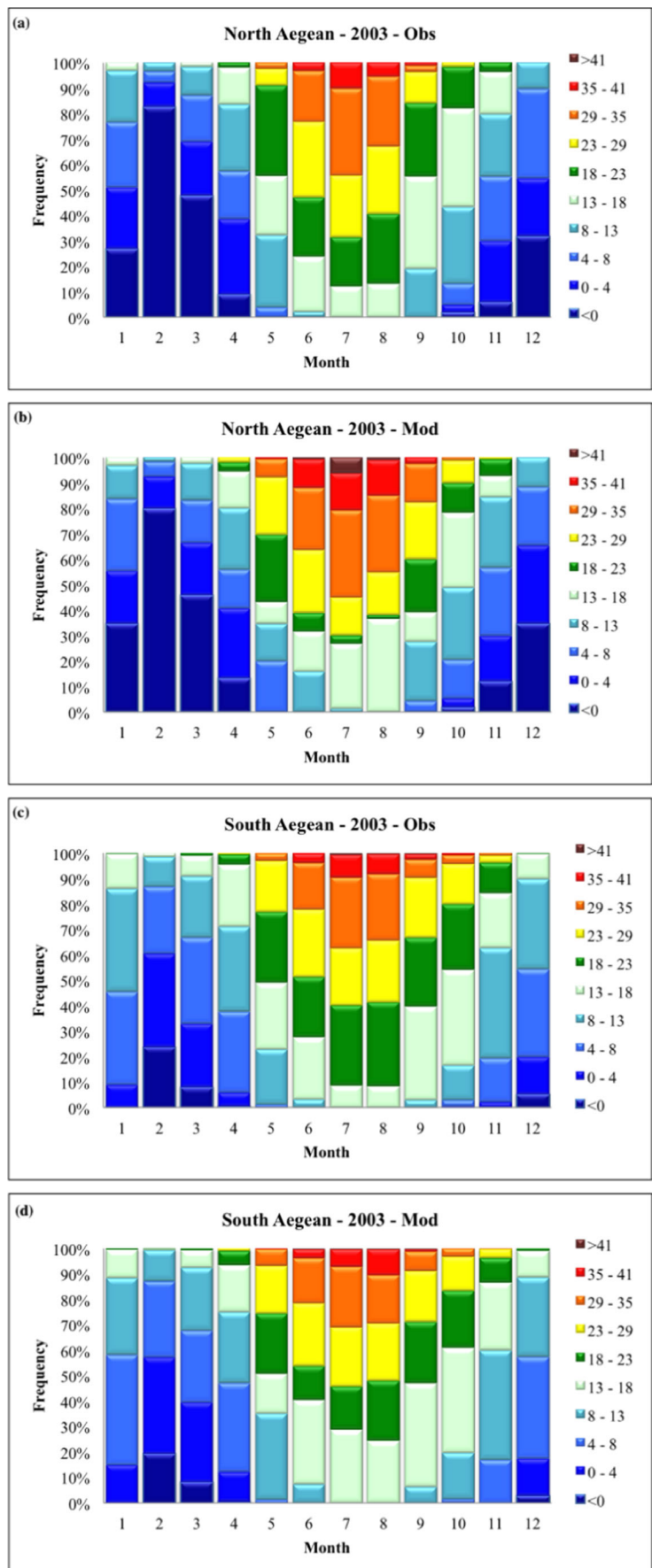
months are also found to exhibit the highest frequencies, exceeding 50 %, of neutral and near-neutral thermal conditions (13 °C<PET<29 °C). February is modeled and observed to be the month with the most occurrences of extreme cold stress (PET<4 °C). However, the northern part of Greece appears to be more prone to such bioclimatic conditions. According to both model results and observations, during February, about 90 % of the time PET drops below 4 °C in North Greece (Fig. 3a, b) and North Aegean (Fig. 4a, b). This percentage is lower in the case of South Greece (Fig. 3c, d) and South Aegean (Fig. 4c, d), approximating 80 and 60 %, respectively. During the summer period, the north-to-south differentiation of PET is not as strong as in the winter. This is particularly true for the continental country, where the frequencies of strong/extreme heat stress (PET>29 °C) are successfully modeled to be of about the same magnitude in North (~35–45 %, Fig. 3b) and South Greece (~40–55 %, Fig. 3d). Regarding the Aegean Sea, the differences in the frequencies of PET>29 °C between the northern (Fig. 4b) and southern part (Fig. 4d) are modeled to be larger. However, this seems to be primarily due to the overestimation of PET> 35 °C in North Aegean (Fig. 4a, b).

Figure 5 presents the time series of the mean daily PET values at 1200 UTC, at the selected synoptic weather stations. Overall, the model manages to capture successfully the variation of bioclimatic conditions throughout the examined time period, as highlighted by the computed correlation coefficients ($R^2>0.95$, not shown). As seen in Fig. 5a, c, the northern areas of Greece experience midday strong/extreme cold stress (PET<8 °C) for a prolonged period spanning from late October through early April. This period is much shorter in the case of the southern country (Fig. 5b, d). Particularly for South Aegean (Fig. 5d), it can be seen that midday extreme low PET values rarely occur. Although the model appears to underestimate high PET values, mean values over 35 °C, indicating a pronounced thermal stress level, are successfully simulated to occur most frequently in South Greece (Fig. 5b). On the other hand, South Aegean is modeled and observed to exhibit the least occurrences of PET>35 °C.

The previous findings agree well with previous studies of the thermal bioclimate of Greece. For instance, Matzarakis and Mayer (1997) found that cold stress in South Greece occurs mostly from October until April, while heat stress conditions are most frequently observed from June until September. Moreover, the effect of the Etesian wind system on reducing thermal stress in the Aegean Sea region has been reported in previous studies (e.g., Matzarakis and Mayer 1997). This is in good agreement with the current study, reporting South Aegean as the least prone geographical area to heat stress during the summer.

As a synthesis of the previously reported results, Fig. 6 presents the modeled spatial distribution of the number of days characterized by strong cold stress (PET<10 °C) and strong heat stress (PET>30 °C) at 1200 UTC during January (Fig. 6a) and July (Fig. 6b), respectively. The particular time of the day for which the corresponding data are shown has been already justified, while the selection of the 2 months aims at contrasting wintertime and summertime conditions.

Under both wintertime and summertime conditions, it can be seen that the spatial variation of days with PET<10 °C (Fig. 6a) and PET>30 °C (Fig. 6b) correlates pretty well with the spatial variations of topography (Fig. 1b). For instance, the most mountainous regions of Greece are characterized for the highest number of days with strong cold stress conditions (Fig. 6a), whereas during summer, they are found to exhibit the least days with strong heat stress conditions (Fig. 6b). In agreement with past studies (e.g., Matzarakis and Mayer 1997), it is found that the inner parts of the Greek mainland are the most prone to high PET values, contrary to the islands of the Aegean Sea where the number of days with strong heat conditions is generally lower (Fig. 6b).

Determinants of the thermal bioclimate

To evaluate the influence of environmental factors on the thermal bioclimate of Greece, correlation matrices of air temperature (TA), vapor pressure (VP), cloud cover (CC), wind speed (WS), and mean radiant temperature (TMRT) against PET were constructed. The investigation of the intercorrelation between the selected thermal index and the meteorological parameters was carried out into two stages. First, the determinants of the daytime (1200 UTC) and nocturnal (0300 UTC) thermal bioclimate were investigated (Table 5). At a second stage, the 1200 UTC winter (DJF) and summer (JJA) subsets of data were used for examining the determinants of strong cold stress (PET<10 °C) and strong heat stress (PET>30 °C), respectively (Table 6). The selection of the time period has been previously justified as representing the most favorable conditions in winter and the worst in summer. The presented results (Tables 5 and 6) refer to the regional groups of stations that were previously defined, although similar results were obtained for the rest of the stations.

TA and TMRT appear to be the variables with the greatest influence on PET during both day and night (Table 5). In particular, the numerical simulations, in good agreement with the observations, indicate a slightly more pronounced influence of air temperature ($R^2>0.95$) as compared to that of mean radiant temperature ($R^2<0.95$). VP is found to be the meteorological parameter with the third greatest impact on PET. As seen in Table 5, the impact of VP is successfully simulated to be more pronounced during the night ($R^2>0.80$) than during the day ($R^2<0.80$). Contradicting daytime and nighttime, the most striking feature is found to be the impact of CC. Clearly, CC appears to influence PET values to a greater extent during the daytime than during the night. As regards WS, its influence on thermal stress is found to be less pronounced than that
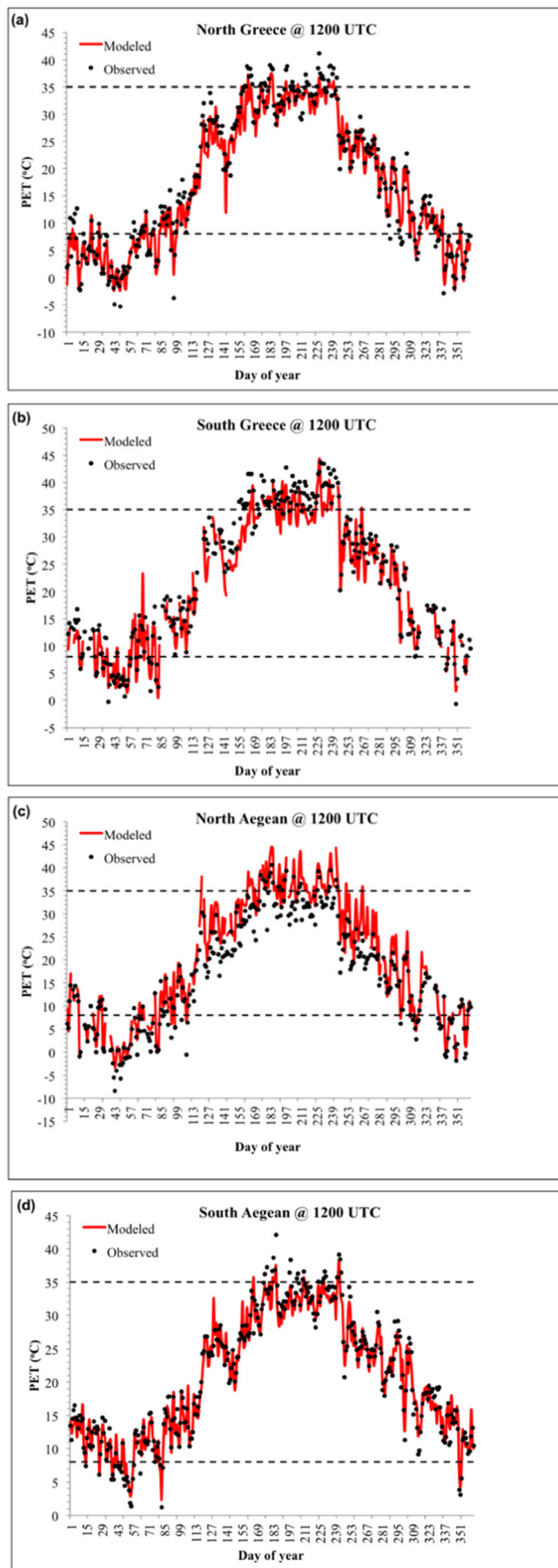
◀ **Fig. 5** Modeled (*lines*) and observed (*points*) mean daily values of PET at 1200 UTC for **a** North Greece, **b** South Greece, **c** North Aegean, and **d** South Aegean, for the year 2003. *Dashed lines* denote the levels of strong/extreme cold (PET<8 °C) and strong/extreme heat (PET>35 °C) stress

of the other variables (Table 5), although the model generally overestimates its importance.

Looking at Table 5, one can finally notice that the determinants of PET are, more or less, common to all examined sites, irrespective of the geographical group they belong to. This is particularly true for the key variables of TA and TMRT, as well as for VP.

Although the model appears to generally underestimate the importance of TMRT in determining extreme PET values, the relative significance of the examined meteorological variables is adequately reproduced (Table 6). According to both the numerical simulations and observations, TA is the key determinant of PET<10 °C in the winter, followed by VP and WS, whereas TMRT is found to play a less pronounced role (Table 6), possibly due to the reduced incoming solar radiation. Not surprisingly, the importance of TMRT increases significantly in the summer. As seen in Table 6, strong heat stress conditions (PET> 30 °C) are mostly determined by TMRT and TA. Contrary to what has been modeled and observed for the winter, VP is now found to have a negligible contribution (R^2<0.10) to summer PET values exceeding 30 °C. As for the WS, the data presented in Table 6 suggest a lower impact on PET>30 °C than on PET< 10 °C values. Nevertheless, it can be seen that the numerical simulations tend to overestimate its significance.

Discussion

The study of the thermal bioclimate can provide useful information for decision making on various levels including health, tourism, and regional planning. Numerical models, which can be coupled with human-response models, are considered to be one valuable tool for this purpose. In the present study, the meteorological WRF model and the human-response model RayMan are synergistically used to assess the thermal bioclimate of Greece during a 1-year time period. This represents a valuable step for identifying the strengths and weaknesses of numerical modeling techniques in terms of reproducing thermal bioclimatic conditions. This kind of information could be exploited for improving regional model simulations, an issue of particular importance for regions such as the Mediterranean, where the projected climate change is expected to significantly deteriorate thermal bioclimate (Matzarakis and Nastos 2011).

The validation of the model-simulated thermal bioclimate, using synoptic weather station data and selecting PET as an

Fig. 6 Modeled number of days: **a** with strong cold stress conditions (PET<10 °C) during January 2003 and **b** with strong heat stress conditions (PET> 30 °C) during July 2003
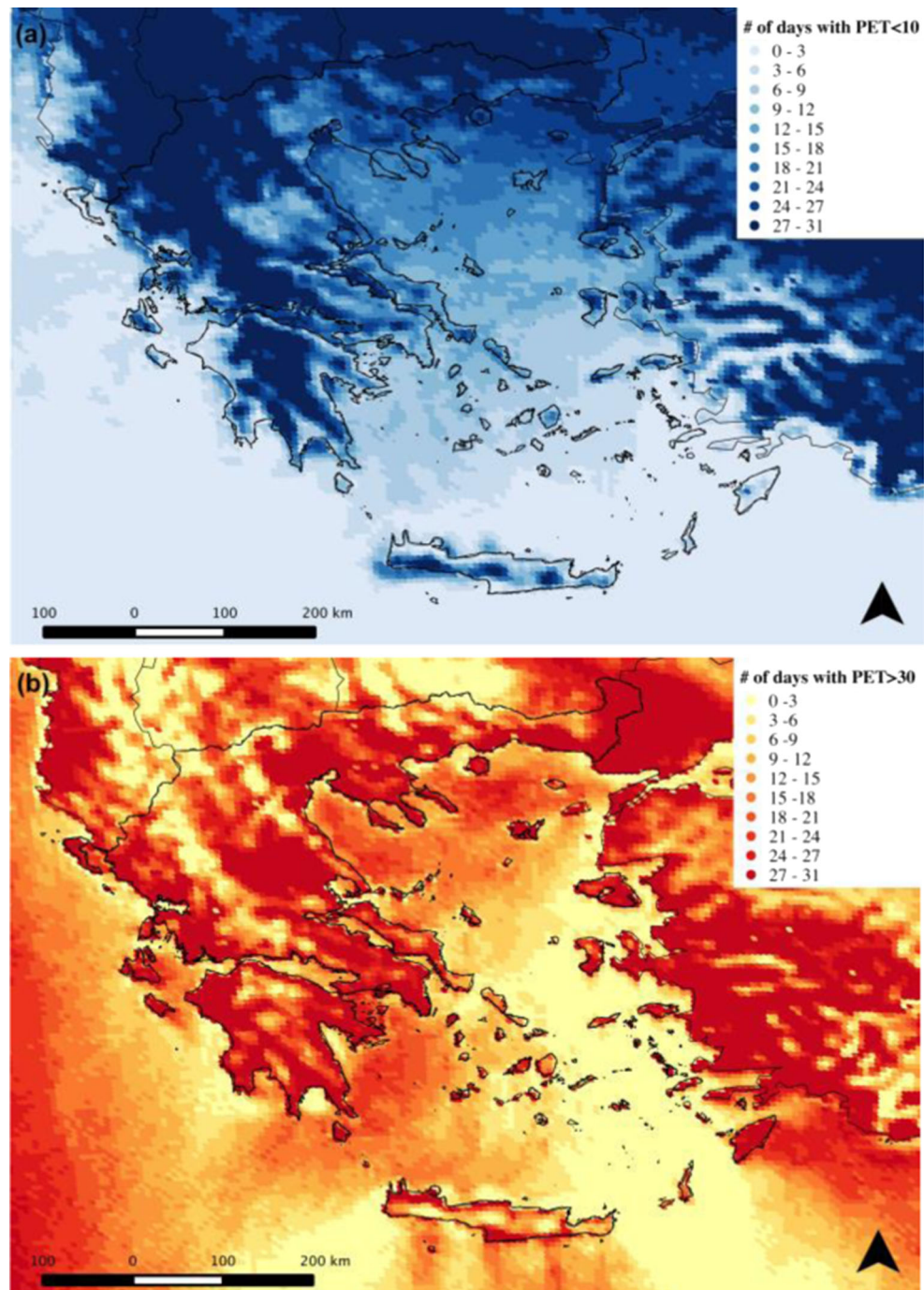
index, suggests an overall satisfactory model performance. The comparison between the WRF-modeled and observed PET values revealed a rather good level of agreement, characterized by mean biases that did not exceed 1.5 °C and RMSE values lower than 4 °C. The general pattern of the seasonal variation of thermal bioclimatic conditions was reproduced adequately well, in agreement with both the observations and earlier studies (e.g., Matzarakis and Mayer 1997). The WRF simulations have also proven to be

successful in terms of replicating the temporal variations of midday extreme PET values.

Despite the positive sides, the conducted analysis also revealed particular weaknesses in the adopted numerical modeling approach. Most importantly, it was found that the WRF-simulated thermal bioclimate is systematically biased cold. Additionally, results indicate that the model's biases exhibit both seasonal and geographical dependence.

Table 5 Modeled and observed correlation coefficients (R^2) between PET and meteorological parameters in the daytime (1200 UTC) and nighttime (0300 UTC). All correlation coefficients are statistically significant ($\alpha=0.05$)

Region	Correlation matrix										
	Time period	TA		VP		CC		WS		TMRT	
		Obs	Mod	Obs	Mod	Obs	Mod	Obs	Mod	Obs	Mod
North Greece	Daytime	0.98	0.97	0.69	0.77	0.22	0.15	0.08	0.18	0.94	0.93
	Nighttime	0.99	0.99	0.81	0.89	0.06	0.00	0.06	0.15	0.94	0.93
South Greece	Daytime	0.98	0.96	0.50	0.57	0.46	0.24	0.02	0.20	0.93	0.92
	Nighttime	1.00	0.99	0.78	0.89	0.33	0.20	0.02	0.21	0.91	0.92
North Aegean	Daytime	0.98	0.97	0.66	0.55	0.42	0.33	0.15	0.30	0.91	0.94
	Nighttime	0.99	0.99	0.89	0.89	0.30	0.08	0.18	0.21	0.91	0.89
South Aegean	Daytime	0.97	0.93	0.52	0.65	0.39	0.22	0.02	0.10	0.89	0.88
	Nighttime	0.99	0.97	0.73	0.85	0.26	0.07	0.04	0.09	0.87	0.88

Summertime meteorological conditions have proven to be harder to model, resulting to considerably underestimated PET values. In particular, the differences between the WRF-simulated and observed PET were found to be larger for the higher values than for the lower values. Part of this uncertainty could be due to the underestimation of air temperature, which tends to be more pronounced during the warm part of the year. For instance, Katsafados et al. (2011) reported greater cold biases in their WRF simulations of air temperature over Greece during the summer than during the winter. Giannaros et al. (2013a) and Miao et al. (2007) also documented the underestimation of air temperature in their mesoscale numerical simulations.

Besides the underestimation of air temperature, the results of this study suggest uncertainties in the computation of mean radiant temperature, which plays a key role in determining summertime thermal bioclimatic conditions. The lower than observed WRF-simulated PET indicates that the mean radiant temperature is underestimated. This underestimation could be, at least partially, attributed to the uncertainties in the modeled air temperature, which influences the computation of long-wave radiation fluxes within RayMan (Matzarakis et al. 2010). Another contributing factor could be the WRF-modeled cloud cover. Uncertainties in the simulation of cloud cover (e.g., Lara-Fanego et al. 2012) are expected to influence the RayMan-simulated global radiation and, thus, the mean radiant temperature (Matzarakis et al. 2010).

Another important factor that should be also included at this juncture of discussion is the potential impact of wind speed on the computed PET values. Recently, Giannaros et al. (2013b) reported that WRF tends to overestimate wind speed, in particular over the Aegean Sea. Higher than the

Table 6 Modeled and observed correlation coefficients (R^2) between the specified PET classes and meteorological parameters at 1200 UTC. The winter (DJF) and summer (JJA) subsets of data have been used for the PET<10 °C and PET>30 °C classes, respectively. All correlation coefficients are statistically significant ($\alpha=0.05$)

Region	Correlation matrix										
	PET classes	TA		VP		CC		WS		TMRT	
		Obs	Mod	Obs	Mod	Obs	Mod	Obs	Mod	Obs	Mod
North Greece	PET<10 °C	0.88	0.73	0.45	0.26	0.01	0.00	0.18	0.57	0.36	0.21
	PET>30 °C	0.88	0.75	0.07	0.01	0.05	0.00	0.08	0.16	0.85	0.62
South Greece	PET<10 °C	0.83	0.78	0.35	0.30	0.02	0.01	0.21	0.43	0.12	0.14
	PET>30 °C	0.77	0.53	0.02	0.15	0.10	0.00	0.05	0.40	0.96	0.67
North Aegean	PET<10 °C	0.93	0.95	0.58	0.50	0.07	0.01	0.42	0.25	0.17	0.33
	PET>30 °C	0.68	0.76	0.01	0.04	0.03	0.00	0.30	0.32	0.82	0.85
South Aegean	PET<10 °C	0.77	0.66	0.28	0.39	0.00	0.01	0.22	0.22	0.16	0.20
	PET>30 °C	0.80	0.80	0.09	0.05	0.02	0.09	0.19	0.01	0.88	0.78

observed model-simulated wind velocities could result to underestimated PET values. This seems to be confirmed in this study, especially if one looks at the simulated thermal bioclimate for the Aegean Sea. In particular, the overestimation of the occurrences of low PET values could be due to the overestimated wind regime of this particular geographical region (Giannaros et al. 2013b).

The results of this study indicate that numerical modeling can provide a useful tool for the assessment of the thermal bioclimate. The meteorological WRF model, in particular, appears to be one attractive solution for this problem. As it was shown and discussed, it is capable of reproducing the key features of the thermal bioclimate of the complex Greek territory. However, there is still room for developments in order to address the previously discussed inadequacies. Most importantly, we should focus on improving the quality of numerical forecasts. This is considered to be critical for allowing for a more accurate representation of the environmental conditions determining the thermal bioclimate. An in-depth analysis of the meteorological model's schemes and parameterizations, conducting sensitivity cases studies, could contribute toward this direction. In addition, increasing the horizontal resolution of the simulations should be also examined as a potential method for improving model performance.

Conclusions

In the present study, the thermophysiologically significant evaluation of the thermal environment of Greece was accomplished by means of coupling a state-of-the-art numerical weather prediction model, namely the WRF, with the model RayMan in order to compute PET. Synoptic weather station data were used for evaluating the model performance. Despite the reported deficiencies, the presented approach showed good adequacy in replicating the thermal bioclimate of the study area during a 1-year time period. Overall, PET was simulated well by the WRF model. The model was found to perform better over the relatively simple terrain of insular Greece than over continental Greece, which suggests that a higher horizontal resolution may be required for improving the accuracy of the numerical simulations.

The importance of the current study is not just limited to investigating the ability of a particular numerical weather prediction model in terms of reproducing the meteorological conditions that together determine the thermal bioclimate. Numerical models, such as the one used in this study, could be employed to serve a variety of purposes in the context of human biometeorology. These purposes vary from integrating the prediction of thermophysiologically significant indices into operational weather forecasting activities, to conducting case studies for supporting urban planning and tourism development. For this, numerical weather prediction models should

be continuously evaluated in order to identify the required developments for improving the simulation of thermal bioclimate.

References

Charalampopoulos I, Tsiros I, Chronopoulou-Sereli A, Matzarakis A (2013) Analysis of thermal bioclimate in various urban configurations in Athens, Greece. Urban Ecosyst 16:217–233

Chen F, Dudhia J (2001) Coupling an advanced land-surface/hydrology model with the Penn State/NCAR MM5 modeling system. Part I: Model description and implementation. Mon Weather Rev 129:569–585

CIA (2013) The World Factbook 2013–14, Central Intelligence Agency, Washington DC (Available online at: https://www.cia.gov/library/publications/the-world-factbook/index.html; last accessed on April 4 2014)

De Freitas CR, Matzarakis A, Scott D (2007) Climate, tourism and recreation: a decade of the ISB's commission on climate, tourism and recreation. In Proceedings 3rd International Workshop on Climate, Tourism and Recreation, 19–22 September 2007, Alexandroupolis, Greece

Dudhia J (1989) Numerical study of convection observed during the winter monsoon experiment using a mesoscale two-dimensional model. J Atmos Sci 46:3077–3107

Endler C, Matzarakis A (2011) Analysis of high-resolution simulations for the Black Forest region from a point of view of tourism climatology—a comparison between two regional climate models (REMO and CLM). Theor Appl Climatol 103:427–440

Fanger PO (1972) Thermal comfort. McGraw-Hill, New York

Fröhlich D, Matzarakis A (2013) Modeling of changes in thermal bioclimate: examples based on urban spaces in Freiburg, Germany. Theor Appl Climatol 111:547–558

Gagge AP, Fobelets AP, Berglun LG (1986) A standard predictive index of human response to the thermal environment. ASHRAE Trans 92:709–731

Giannaros TM, Melas D, Daglis IA, Keramitsoglou I (2013a) Numerical study of the urban heat island over Athens (Greece) with the WRF model. Atmos Environ 73:103–111

Giannaros TM, Melas D, Ziomas, I (2013b) Performance evaluation of a mesoscale modeling system for wind resource assessment. 13th International Conference on Environmental Science and Technology, 5–7 September 2013, Athens, Greece

Gulyás A, Unger J, Matzarakis A (2006) Assessment of the microclimatic and human comfort conditions in a complex urban environment: modeling and measurements. Build Environ 41:1713–1722

Hong SY, Lim JOJ (2006) The WRF single-moment 6-class microphysics scheme (WSM6). J Korean Meteor Soc 42:129–151

Höppe PR (1984) Die Energiebilanz des Menschen. Dissertation, Wissenschaftliche Mitteilungen des Meteorologischen Instituts der Universität München 49

Höppe PR (1993) Heat balance modeling. Experientia 49:741–746

Höppe PR (1999) The physiological equivalent temperature—a universal index for the biometeorological assessment of the thermal environment. Int J Biometeorol 43:71–75

ISO (1982) ISO 7243: hot environments—estimation of the heat stress working man based on WBGT index (Wet Bulb Globe Temperature). International Organization of Standardization, Geneve

Janjic ZI (1994) The step-mountain eta coordinate model: further developments of the convection, viscous sublayer and turbulence closure schemes. Mon Weather Rev 122:927–945

Janjic ZI (1996) The surface layer in the NCEP Eta model. 11th Conference on Numerical Weather Prediction, 19–23 August 1996, Norfolk, VA, USA

Janjic ZI (2002) Nonsingular implementation of the Mellor-Yamada level 2.5 scheme in the NCEP meso model. NCEP Office Note 437, 61 pp

Kain JS (2004) The Kain-Fritsch convective parameterization: An update. J Appl Meteorol 43:170–181

Katsafados P, Papadopoulos A, Mavromatidis E, Gikas N (2011) Quantitative verification statistics of WRF predictions over the Mediterranean region. 12th Annual WRF Users' Event, 20–24 June 2011, Boulder CO

Lara-Fanego V, Ruiz-Arias JA, Pozo-Vazquez D, Santos-Alamillos FJ, Tovar-Pescador J (2012) Evaluation of the WRF model sola irradiance forecasts in Andalusia (southern Spain). Sol Energ 86:2200–2217

Matzarakis A (2006) Weather- and climate-related information for tourism. Tourism Hospit Plann Dev 3(2):99–115

Matzarakis A, Mayer H (1996) Another kind of environmental stress: thermal stress. WHO Newsletter 18:7–10

Matzarakis A, Mayer H (1997) Heat stress in Greece. Int J Biometeorol 41:34–39

Matzarakis A, Nastos P (2011) Human-biometeorological assessment of heat waves in Athens. Theor Appl Climatol 105:99–106

Matzarakis A, Rutz F, Mayer H (2007) Modeling radiation fluxes in simple and complex environments—application of the RayMan model. Int J Biometeorol 51:323–334

Matzarakis A, Rutz F, Mayer H (2010) Modeling radiation fluxes in simple and complex environments: basics of the RayMan model. Int J Biometeorol 54:131–139

Mayer H (1993) Urban bioclimatology. Experientia 49:957–963

Mayer H, Höppe P (1987) Thermal comfort of man in different urban environments. Theor Appl Climatol 38:43–49

Miao JF, Chen D, Borne K (2007) Evaluation and comparison of Noah and Pleim-Xiu land surface models in MM5 using GOTE2001 data: spatial and temporal variations in near-surface air temperature. J Appl Meteorol Climatol 46:1587–1605

Mlawer EJ, Taubman SJ, Brown PD, Iacono MJ, Clough SA (1997) Radiative transfer for inhomogeneous atmosphere: RRTM, a validated correlated-k model for the long-wave. J Geophys Res 102(D14):16663–16682

Nastos PT, Matzarakis A (2006) Weather impacts on respiratory infections in Athens, Greece. Int J Biometeorol 50:358–369

Papangelis G, Tombrou M, Dandou A, Kontos T (2012) An urban "green planning" approach utilizing the Weather Research and Forecasting (WRF) modeling system. A case study of Athens, Greece. Landscape Urban Plan 105:174–183

Parsons K (1993) Human thermal environments. Taylor & Francis, London

Shiue I, Matzarakis A (2011) Estimation of the tourism climate in the Hunter Region, Australia, in the early twenty-first century. Int J Biometeorol 55:565–574

Skamarock WC, Klemp JB, Dudhia J, Gill DO, Barker DM, Duda MG, Huang XY, Wang W, Powers JG (2008) A description of the advanced research WRF version 3. NCAR Technical Note, NCAR/TN-475 + STR, June 2008, Boulder CO, 125 pp

Steadman RG (1971) Indices of wind chill of clothed persons. J Appl Meteorol 10:674–683

Thom EC (1959) The discomfort index. Weatherwise 12:57–60